Guest-Cage Atomic Interactions in a Clathrate-based Phase-Change Material

*Desmond Loke, Jonathan M. Skelton, Leong-Tat Law, Wei-Jie Wang, Ming-Hua Li, Wen-Dong Song, Tae-Hoon Lee, Stephen R. Elliott**

Dr. D. Loke, Dr. J. M. Skelton, Dr. T. H. Lee, Prof. S. R. Elliott
Department of Chemistry, University of Cambridge
Lensfield Road, Cambridge, CB2 1EW, UK
E-mail: sre1@cam.ac.uk

L. T. Law, Dr. W. J. Wang, Dr. M. H. Li, Dr. W. D. Song
Data Storage Institute, A*STAR (Agency for Science, Technology and Research)
DSI Building, 5 Engineering Drive 1, Singapore 117608

Dr. D. Loke
National University of Singapore (NUS) Graduate School for Integrative Sciences and Engineering, 28 Medical Drive, Singapore 117456.

Keywords: nano-engineering, phase-change materials, clathrate compounds, crystallization kinetics, guest-cage interactions

The reliance of future technologies on the development of economical methods for boosting the performance of portable-electronic devices beyond just miniaturization (owing to physical and lithographic constraints) has spurred intense and rapid progress in the area of material nano-engineering[1-3]. Phase-change materials (PCMs) are fast-switching materials, and the ability to design nano-engineered PCMs has led to broad applications in nonvolatile memories[4,5], reconfigurable electronics[6,7] and, more recently, photonic devices[8] and neuromorphic computing[9,10]. PCMs, based on the reversible switching between amorphous (*a*) and crystalline (*c*) phases[11], are generally scalable down to nanometer length scales[12]. The pursuit of nano-engineering methods to enhance the performance of PCMs has yielded strategies including, but not limited to, the formation of superlattices in PCM nanowires[13] and PCM nanoclusters in silica[14]. Although each method has had some success in achieving PCMs with improved properties, no distinct strategy to date has yet focused on 'engineering' the atomic structure of a PCM itself.

One approach for realizing such a material is through the formation of a cage-like structure, requiring an unusual interaction between the guest atoms and host matrix that is commonly found in clathrates[15]. Clathrates are compounds formed by the inclusion of atoms or molecules (guests) into the cages of a matrix (host) formed by other components[15]. The ability to control the interactions between the guest atoms and the host matrix of clathrates has proven to be a viable means to alter the properties of such materials on the nanoscale. The exploitation of clathrates has led to the discovery of new materials that have, for instance, demonstrated control over thermal conductivity[16] and crystal nucleation[17], or the ability to store and release biomolecules[18]. Since these diverse processes are, at the fundamental level, linked to the interactions between the guest atoms and the host matrix, the material properties can be easily controlled, for instance, by varying the type and concentration of the guest species.

We report here the formation of new clathrate forms of a PCM, based on cage frameworks, which allows for altering the crystallization, as well as amorphization, by controlling the interactions between the guest atoms and the host matrix via 'inter-complex' guest-atom vibrations. The formation of a PCM with cage-like structures (PCM-CLS) using two chemically different elements, viz. Cs and Ba, as the guest atoms in the archetype PCM, $Ge_2Sb_2Te_5$ (GST) as host, demonstrates both the flexibility of the cage scaffold, and the ability precisely to control the material characteristics through guest-atom modifications. In contrast to other nano-engineering methods, this approach allows for the nanoscopic control of crystallization of PCMs using a universal cage template based on the incorporation of alkali or alkaline-earth ions.

We employed *ab initio* molecular-dynamics (AIMD) simulations to investigate the structural properties of, and interactions between, the guest atoms and the host matrix using four models of doped GST. The first three models, denoted C′, C″ and C‴, had one, two and three Cs guest atoms in a GST matrix formed by thirteen Ge, thirteen Sb, and thirty-five, thirty-four and thirty-three Te atoms, respectively, while a fourth model (B″) had two Ba guest atoms in a GST matrix formed by thirteen Ge, thirteen Sb, and thirty-four Te atoms. The compositions of the models were predefined, based on a material compositional study (see supporting information). The models were generated with initial densities of around 6.07 g cm^{-3}, chosen to be close to the experimental *a*-phase density of GST[19]. The AIMD simulations were carried out using the VASP code[20] (see supporting information). Random initial configurations were equilibrated as liquids at 1000 K for 180 ps, followed by thermal quenching to 300 K at a rate of dT/dt = -25 K ps^{-1} to generate the *a*-models. To study the dynamics of the guest atoms, indicative of their interactions with the host matrix, the models were annealed at 300 K for 30 ps. The models were then relaxed at 0 K to examine their structural properties.

Figure 1 shows a snapshot of a Cs-doped *a*-model, along with an equivalent mass-spring model, and partial radial atomic distribution functions ($g(r)$). According to the metal-chalcogenide framework model[21], the incorporation of large electropositive ions, such as alkali or alkaline-earth atoms, into a chalcogenide material should yield a structure that is stabilized by metal-encapsulating cages due to the high-coordination sites which the metal ions adopt, and the ionic character of the surrounding metal-chalcogen bonds. We find that all doped GST models form one or more "cage(s)" within the GST matrix, with each cage enclosing a Cs or Ba atom. The cages were mainly comprised of Te atoms, which was evident from snapshots of the models (see Figure 1a), as well as the pronounced peak in the $g(r)$s between the Cs/Ba and Te atoms, as shown in Figure 1c. The average number of Te atoms forming a cage can be estimated from the area under the first peak in the guest-atom-centred $g(r)$, which gives the average coordination numbers, N_c, for both Cs and Ba atoms to be between 9 and 10, indicating their preference to occupy high-coordination sites, as predicted by the metal-chalcogenide theory. The interatomic separations, r_0, between the Cs/Ba guest and host Te atoms were estimated from the positions of the first peak in $g(r)$, and were found to be between 3.5 and 4.0 Å. These values are very similar to those observed in most Cs/Ba-Te compounds[22,23], confirming the ionic nature of the dopant environments in the doped models. The average r_0 values between Ge or Sb atoms and Te atoms (~3.0 Å) in the host matrix were identical to those observed in undoped GST[24].

We find that the guest atoms exhibit large thermal vibrations. **Figure 2**a shows the squared displacements (SDs) which are averaged over a specific type of atoms during annealing for the doped models at 300 K, whereby the maximum fluctuation found in SD is denoted by Δx_0^2. While the guest atoms in the B″ models exhibit a large Δx_0^2 value of 1.13 Å^2, the host atoms show much smaller Δx_0^2 values of around 0.22 Å^2 (see supporting Table S1). This behaviour is also observed for the three Cs-doped models. We compared the Δx_0^2 values

for the Cs and Ba atoms in the C″ and B″ models, respectively. The calculations show that the $\mathrm{D}x_0^2$ value for the Cs atoms (~2.98 Å^2) is even larger than that for the Ba atoms. This suggests that the vibrational properties of a PCM can be varied by using different types of guest atoms to control the electrostatic interaction (EI) between the guest atoms and host matrix; in this case, the divalent cation, Ba^{2+} has a stronger EI than the univalent cation, Cs^+. In addition, we find that the $\mathrm{D}x_0^2$ value depends on the concentration of the guest atoms, with a higher concentration of Cs atoms leading to a reduction in its amplitude, which suggests that a higher number of guest atoms would lead to a more rigid structure. It should be noted that the characteristic large displacement of Cs and Ba atoms might be investigated experimentally by employing neutron scattering or photon correlation spectroscopy, which could provide an insight into the mean-square relative displacement (MSRD) of the atoms in the matrix[25].

To evaluate the origin of these vibrations, we examined the dynamical behaviour of the guest atoms. The dynamics of the guest-cage interaction can be described in terms of a mass-spring model (Figure 1b), whereby a mass vibrates within a cavity defined by the walls of a cage, which themselves are flexible. We find that the vibrations stemmed from a pronounced movement of the guest atoms between different regions of their cages, with a general movement from sites forming complexes with a low number of host atoms to those formed by a high number of host atoms (see Figure 2b). This motion is likely to be associated with the thermal fluctuations that distort the guest-host bonds, while the apparent preference for a higher coordination is possibly due to the more favourable electrostatic forces acting on the guest atoms in the complexes. The form of the cages was dynamic; it would evolve and change, both in size and position, with time due to thermal motions within the host matrix. In most cases, separate regions of the cages would expand and contract interchangeably, and this mechanism induces the atoms to “rattle” back and forth between the complexes, providing an explanation for the vibrations observed in Figure 2a.

The frequency, v_0, of these guest-cage atomic vibrations is low. According to the loose-cage/tight-cage framework picture[26], some guest atoms do not fit comfortably in a single substitutional site. In general, a guest atom occupies the lowest energy position that is a compromised between an optimum distance at some points of contact with the host matrix, and a less-than-optimum distance at other points of contact. The host matrix tends to distort the guest atom to fit into the available cage, and the extent to which the guest atom is distorted depends on the EI between the guest atom and host matrix. Guest atoms with a strong EI usually find themselves in "tight cages", exhibiting high v_0 values, while those with a weak EI find themselves in "loose cages" exhibiting low v_0 values. Figure 2c shows the averaged partial vibrational density of states (VDOS) for a guest atom in the doped models. The spectra for the C′, C‴ and B″ models are shown, as they display clearer peaks. The Cs and Ba atoms both show low v_0 values, with two peaks in the spectra located at around 1 and 3 THz, which indicate that both atoms do not exhibit very strong EIs, and are likely to be confined in loose cages. The spectra for the Ge, Sb and Te atoms in the host matrix were similar to those for undoped GST and other PCMs[27] (see supporting Figure S1). Aggregation effects[28], which occur as a result of interference from the vibrations of adjacent atoms, typically leads to spectral broadening. This effect is observed as the concentration of the guest atoms was increased; the widths of both peaks in the spectrum for the C‴ model were relatively broader than that for the C′ model. This means that, at high concentrations, the vibrations of the guest atoms are more tightly coupled to those of the host, suggesting the formation of smaller, more tightly-bound cages.

Experimental results for doped GST samples, obtained under similar conditions to those employed in the simulations, are shown in **Figure 3**. To study the influence of the guest atoms on the switching properties, two Ba-doped GST (BGST) film samples, denoted as B1 and B2, with Ba concentrations of 1.4 at% and 4.5 at%, respectively, were fabricated and examined

(see supporting information). For comparison, a pure GST film sample (B0) was also fabricated. The initial electrical resistance, *R*, of the samples was around 100 MΩ. To investigate the properties of the *a*-phase films, the samples were initially studied at 300 K. Because the switching effects at low *T* were too slow to be observed, the samples were examined at gradually increasing *T* at a rate of 0.17 K/s, as well as at a constant *T* = 410 K.

Figure 3a shows the correlation between *R* and *T* of the samples during annealing from 300 K to 470 K. The samples show a reduction in *R* from 100 MΩ to 10 kΩ over this range of *T* due to structural ordering of the *a*-phase matrix[29]. A sharp drop in the *R* level, from 1 MΩ to 10 kΩ, was observed at an onset temperature (T_{on}) of about 420 to 450 K, which indicates that the films had transformed in an $a \rightarrow c$ phase transition. The value T_{on} provides a measure of the thermal energy E_T required for the phase transition. We find that both BGST films required a higher E_T to switch than that for the GST film, as manifested by the B1 and B2 samples having higher T_{on} values of 425 K and 440 K, respectively, compared to 415 K for the B0 samples, suggesting that the energy required to induce a phase transition, and hence the thermal stability of the *a* phase, can be controlled by altering the guest-atom concentration.

The BGST samples exhibit long-term *a*-phase stability. This was observed via the time-dependence of *R* during annealing at 410 K (see Figure 3b). The initial *R* value for the samples was lower than that observed in Figure 3a, as the starting *T* employed in this experiment was higher. For both B0 and B1 samples, *R* decreased from around 10 MΩ to 100 kΩ within 600 s of annealing. While the B0 sample shows a sharp drop in *R*, indicative of an $a \rightarrow c$ phase transition, which occurred after an onset time t_{on} = 20 s, the B1 sample exhibits a much longer t_{on} = 400 s. The B2 sample maintained a high and constant *R* value of 10 MΩ throughout the test period. These results indicate that the guest atoms promote stability of the *a*-phase, and that higher concentrations of guest atoms lead to longer retention times.

Finally, the BGST films show a reduction in melting energy, high recrystallization speed, as well as clear reversibility of the phase transition. In addition, based on the AIMD simulations, they also exhibit a small change in density for the $a \rightarrow c$ phase transition (Figures 3c-e; see also supporting information). These results demonstrate further the potential utility of these materials for device applications.

Both experimental and simulation results suggest that the enhanced *a*-phase stability may stem from the presence of the guest atoms, leading to a more rigid *a*-structure. At low *T*, the large coordination cage and strong electrostatic interactions between the guest and the host atoms, evident from the AIMD simulations, will restrict atomic diffusion, which is required for structural ordering. This phenomenon would explain both the observed higher T_{on}, and also the longer t_{on}, seen in the BGST samples. The combined use of experiments, theoretical modeling, and simulations further infer that the BGST films in the *c* phase should exhibit a cage-like structure (Figures S4, S5; see also supporting information). According to Slack's "rattler-atom" theory[30], the motion of guest atoms produces low-frequency anharmonic phonon modes, which can scatter heat-carrying acoustic modes, and thereby reduce the thermal conductivity of the material. It is plausible that the BGST films have lower thermal conductivities than the GST films, which allows them to switch from the $a \rightarrow c$ phase with a low E_T. It is, however, noted that T_m increases with Ba concentration, possibly due to the rattling motion being suppressed at high guest-atom concentrations, as suggested by the AIMD simulations (see Figure 2a).

According to the resonance-bonding theory, an increase in the ionic character in the bonding of a PCM should induce a weaker delocalization of charge carriers, which yields a smaller change in its optical properties (e.g. optical contrast, absorption redshift) between the *a* and *c* phases, as well as an associated decrease in its electronic properties (e.g. electronic polarizability, electrical conductivity) in the *c* phase [31-34]. Figure 3f shows a plot of the

change in the optical reflectivity r of the BGST samples as a function of temperature. The change in r of a sample, normalized with respect to its full $a \rightarrow c$ phase transition, is given by $\Delta r/r_n = (r\text{-}r_i)/(r_m\text{-}r_i)$, where r_n, r, r_i, and r_m are the normalized, point, initial and maximum reflectivities of the sample. We find that the BGST films show a weaker delocalization of charges than for undoped GST, as manifested by the smaller $\Delta r/r_n$ values exhibited by the B1/B2 samples compared to that for the B0 sample upon an $a \rightarrow c$ phase transition, for instance, between T = 500 K and T = 700 K. The same phenomenon is also observed from the dependence of the concentration of the charge carriers (holes) on the type of film samples (Figure S6), whereby the B1/B2 samples show a lower carrier concentration than for the B0 sample. These indicate that the BGST films, as is intuitively expected, are more ionic in nature than undoped GST, and that the resonance bonding of a host matrix and hence its optical/electrical-conductivity contrast, is tunable via varying the concentration of the guest atoms.

An interesting question is whether the cage structures could be formed in alternative PCMs, where similar guest atoms could interact with other host matrices to produce novel and unusual phenomena. In general, PCMs can be grouped into nucleation (*N*)-dominated and growth (*G*)-dominated types[35], depending on their crystallization mechanisms. A candidate host matrix is AgInSbTe (AIST), which is a *G*-dominated PCM. Its properties differ markedly from those of GST (an *N*-dominated PCM), as characterized by a smaller probability of nucleation at low *T*, and a larger probability of growth at high *T*. This would allow the use of various types of guest atoms and host matrices, as well as their combinations, to open new avenues for optimizing PCM properties.

Supporting Information

Supporting Information is available online from the Wiley Online Library or from the authors.

Acknowledgements

The authors thank L.P. Shi and R. Ji for valuable discussions on the material-characterization studies. We acknowledge financial support by the Engineering and Physical Sciences Research Council (UK). The AIMD simulations were performed using the Cambridge High-Performance Computing Facility. We gratefully thank the Data Storage Institute, A*STAR (Singapore), for the use of their facilities to fabricate and characterize the film samples. D.L. thanks the NUS Graduate School for Integrative Sciences and Engineering for scholarship support.

References

[1] M. S. Gudiksen, L. J. Lauhon, J. Wang, D. C. Smith, C. M. Lieber, *Nature* **2002**, *415*, 617.

[2] R. E. Algra, M. A. Verheijen, M. T. Borgström, L.-F. Feiner, G. Immink, W. J. P. van Enckevort, E. Vlieg, E. P. A. M. Bakkers, *Nature* **2008**, *456*, 269.

[3] K. Tomioka, M. Yoshimura, T. Fukui, *Nature* **2012**, *488*, 189.

[4] M. Wuttig, *Nat. Mater.* **2005**, *4*, 265.

[5] F. Xiong, A. Liao, D. Estrada, E. Pop, *Science* **2011**, *332*, 568.

[6] K. N. Chen, L. Krusin-Elbaum, D. M. Newns, B. G. Elmegreen, R. Cheek, N. Rana, A. M. Young, S. J. Koester, C. Lam, *IEEE Electron Device Lett.* **2008**, *29*, 131.

[7] S.-M. Yoon, S.-W. Jung, S.-Y. Lee, Y.-S. Park, B.-G. Yu, *IEEE Electron Device Lett.* **2009**, *30*, 371.

[8] B. Gholipour, J. Zhang, K. F. MacDonald, D. W. Hewak, N. I. Zheludev, *Adv. Mat.* **2013**, *25*, 3050.

[9] C. D. Wright, Y. Liu, K. I. Kohary, M. M. Aziz, R. J. Hicken, *Adv. Mat.* **2011**, *23*, 3408.

[10] D. Kuzum, R. G. D. Jeyasingh, B. Lee, H.-S. P. Wong, *Nano Lett.* **2012**, *12*, 2179.

[11] S. R Ovshinsky, *Phys. Rev. Lett.* **1968**, *21*, 1450.

[12] S. Raoux, J. L. Jordan-Sweet, A. J. Kellock, *J. Appl. Phys.* **2008**, *103*, 114310.

[13] C. S. Jung, H. S. Kim, H. S. Im, Y. S. Seo, K. Park, S. H. Back, Y. J. Cho, C. H. Kim, J. Park, J.-P. Ahn, *Nano Lett.* **2013**, *13*, 543.

[14] S. J. Shin, J. Guzman, C.-W. Yuan, C. Y. Liao, C. N. Boswell-Koller, P. R. Stone, O. D. Dubon, A. M. Minor, M. Watanabe, J. W. Beeman, K. M. Yu, J. W. Ager III, D. C. Chrzan, E. E. Haller, *Nano Lett.* **2010**, *10*, 2794.

[15] H. M. Powell, *J. Chem. Soc.* **1948**, 61.

[16] R. G. Ross, P. Anderson, G. Bäckström, *Nature* **1981**, *290*, 322.

[17] M. R. Walsh, C. A. Koh, E. D. Sloan, A. K. Sum, D. T. Wu, *Science* **2009**, *326*, 1095.

[18] G. C. R. Ellis-Davies, *Nat. Methods* **2007**, *4*, 619.

[19] W. K. Njoroge, H.-W. Woltgens, M. Wuttig, *J. Vac. Sci. Technol. A* **2000**, *20*, 230.

[20] G. Kresse, J. Hafner, *Phys. Rev. B* **1993**, *47*, 558.

[21] T. J. McCarthy, S.-P. Ngeyi, J.-H. Liao, D. DeGroot, T. Hogan, C. R. Kannewurf, M. G. Kanatzidis, *Chem. Mater.* **1993**, *5*, 331.

[22] P. F. Lang, B. C. Smith, *Dalton Trans.* **2010**, *39*, 7786.

[23] W. S. Sheldrick, M. Wachhold, *Angew. Chem. Int. Ed. Engl.* **1995**, *34*, 450.

[24] W. Welnic, A. Pamungkas, R. Detemple, C. Steimer, S. Blügel, M. Wuttig, *Nat. Mater.* **2006**, *5*, 56.

[25] T. Matsunaga, N. Yamada, R. Kojima, S. Shamoto, M. Sato, H. Tanida, T. Uruga, S. Kohara, M. Takata, P. Zalden, G. Bruns, I. Sergueev, H. C. Wille, R. P. Hermann, M. Wuttig, *Adv. Funct. Mater.* **2011**, *21*, 2232.

[26] G. C. Pimentel, S. W. Charles, *Pure Appl. Chem.* **1963**, *7*, 111.

[27] P. Long, H. Tong, X. Miao, *Appl. Phys. Express* **2012**, *5*, 031201.

[28] K. Consani, G. C. Pimentel, *J. Phys. Chem.* **1987**, *91*, 289.

[29] J. Hegedüs, S. R. Elliott, *Nat. Mater.* **2008**, *7*, 399.

[30] G. A. Slack, Thermoelectric Materials-New Directions and Approaches, edited by T. M. Tritt, G. Mahan, H. B. Lyon, Jr., M. G. Kanatzidis (Materials Research Society, Pittsburgh, PA, 1997), vol. 478, p. 47.

[31] L. Pauling, Nature of Chemical Bond, Cornell University Press, New York, 1939.

[32] K. Shportko, S. Kremers, M. Woda, D. Lencer, J. Robertson, M. Wuttig, *Nat. Mater.* **2008**, *7*, 653.

[33] B. Huang, J. Robertson, *Phys. Rev. B* **2010**, *81*, 081204.

[34] H. W. Ho, W. D. Song, K. Bai, P. S. Branicio, T. L. Tan, R. Ji, L. T. Law, C. M. Ng, L. Wang, *J. Appl. Phys.* **2013**, *114*, 123504.

[35] G.-F. Zhou, *Mater. Sci. Eng. A* **2001**, *304–306*, 73.

Figure captions

Figure 1. Structural characterization of simulated models of $Ge_2Sb_2Te_5$ (GST) with cage-like structures. a) Snapshot of a Cs atom encaged in a GST matrix of model C″. The green, blue, red, and yellow spheres denote Cs, Ge, Sb, and Te atoms, respectively. Bonds are shown between atoms within a range of 3.0 Å. b) A simple spring model comprised of host-cage walls of mass m_0 interconnected by springs with spring constant K_0, and guest atoms of mass m_1 attached to cage walls with springs of spring constant K_1. c) Partial radial distribution functions $g(r)$ for various atomic species in the models.

Figure 2. Simulated dynamics of guest and host atoms. a) Squared displacements (SDs) for guest and host atoms at 300 K. The maximum in SD fluctuations is denoted by Δx_0^2. The separate curves are displaced by a given amount vertically for clarity. b) Snapshots of a Cs guest atom and the GST host matrix in model C″ corresponding to the positions marked x_1 and x_2 in (a). Colour coding of atoms: Cs, green; Ge, blue; Sb, red; Te, yellow. The silver-grey atoms and bonds belong to those species not involved in the motion of the Cs atom. Bonds are shown between atoms within a range of 3.8 Å. c) Normalised partial vibrational densities of states (VDOS) for guest atoms in the models.

Figure 3. Thermal properties of Ba-doped GST. a) Correlation between film electrical resistance and temperature during annealing at a rate of 0.17 K/s. b) Time dependence of the resistance of films during annealing at 410 K. c) Variation of melting temperature with type of film sample. d) Dependence of optical reflectivity on laser exposure time. e) Image of a film sample after switching from the *a* to *c* phases, and back to the *a* phase. f) Plot of change in optical reflectivity (Δr) normalized with respect to full crystallization (r_n), showing crystallization occurring at 420 K, and melting at 800 K.

Figure 1. Loke *et al.*

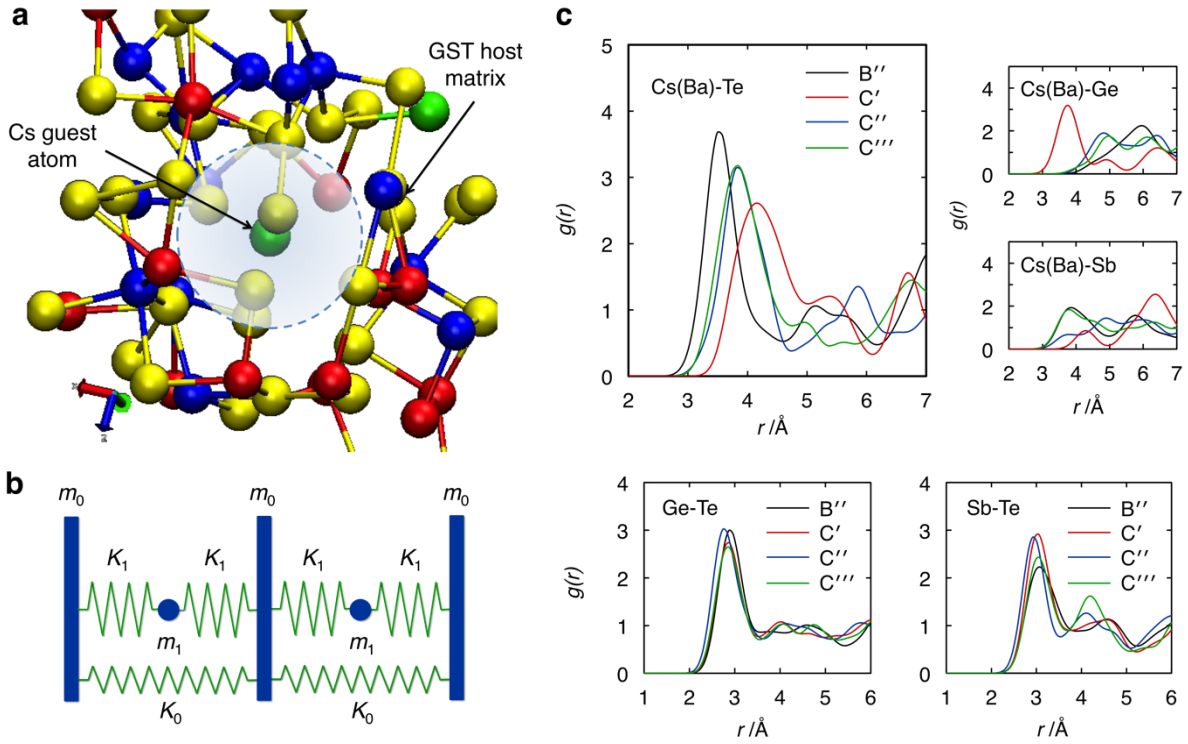

Figure 2. Loke *et al.*

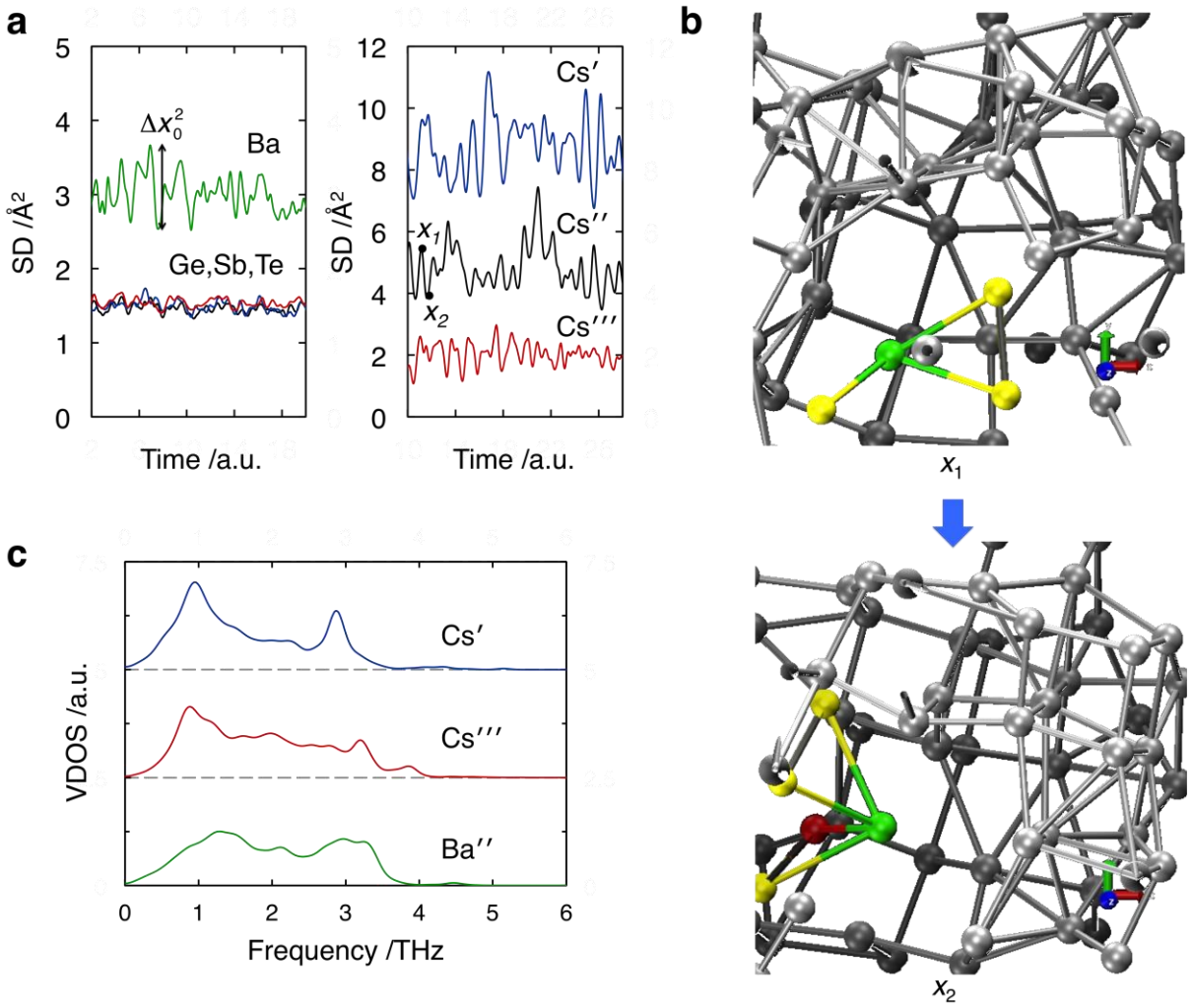

Figure 3. Loke *et al.*

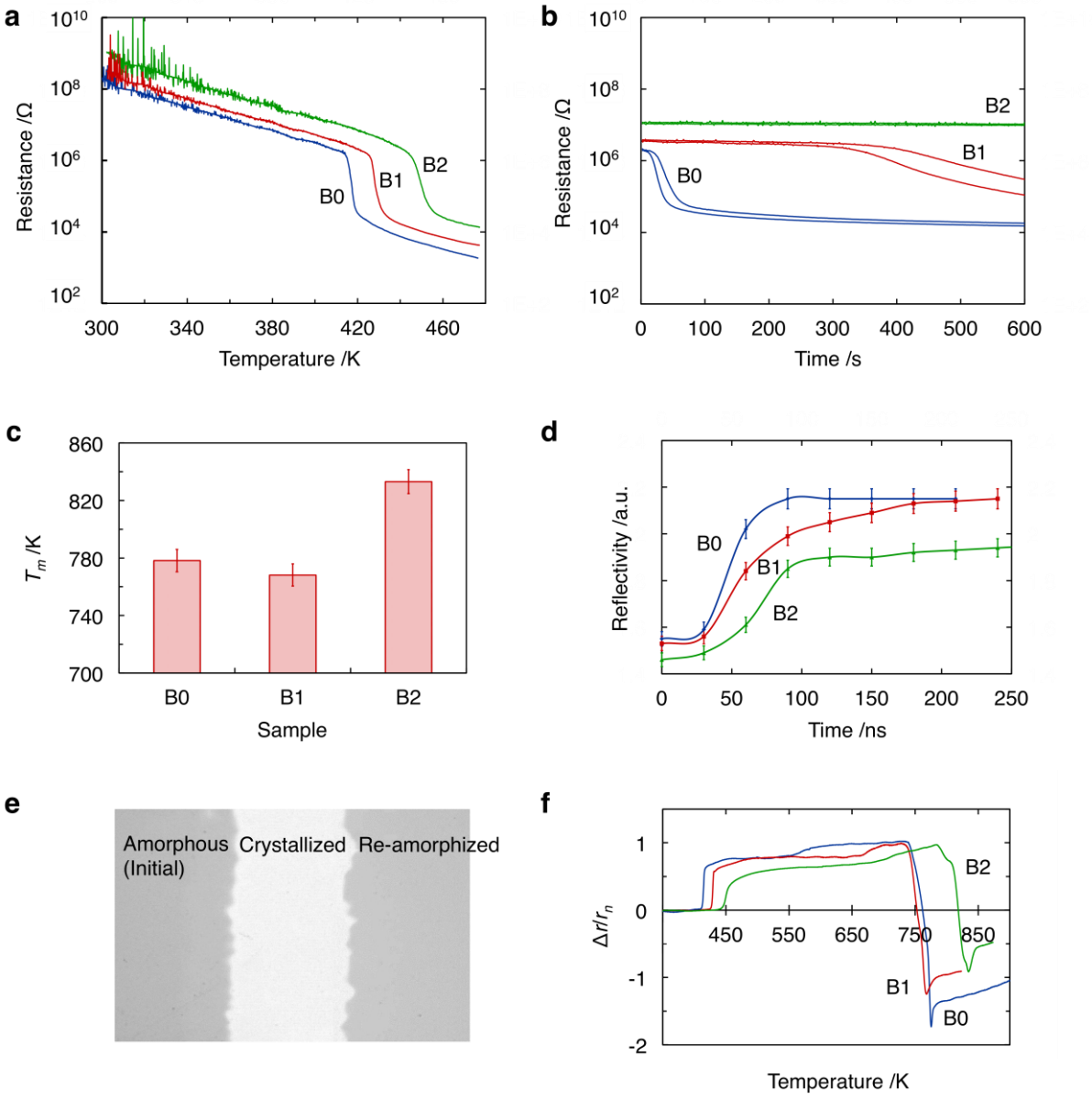

The table of contents entry

We report new clathrate-based, phase-change materials, with cage-like structures incorporating Cs and Ba guest atoms, as a means of altering crystallization and amorphization behaviour by controlling 'guest-cage' interactions via intra-complex guest vibrational effects. Both a high resistance to spontaneous crystallization, and long retention of the amorphous phase were achieved, as well as a low melting energy. This approach provides a route for achieving cage-controlled semiconductor devices.

Keyword (see list)

Desmond Loke, Jonathan M. Skelton, Leong-Tat Law, Wei-Jie Wang, Ming-Hua Li, Wen-Dong Song, Tae-Hoon Lee, Stephen R. Elliott*

Title: Guest-Cage Atomic Interactions in a Clathrate-based Phase-Change Material

ToC figure: